

ENVIRONMENTALLY EFFECTIVE PREPARATION AND CHARACTERIZATION OF CELLULOSE DIACETATE FILM DERIVED FROM WASTE CIGARETTE FILTERS

May Thazin Kyaw¹, Ngwe Sin¹, Aung Than Htwe², Hninn Wutt Yee Htun², Yamin The²

Abstract

Cigarette waste pollutes the environment and is a problem that must be solved. However, such waste can be recycled by converting it into raw materials for the production of new products. The purpose of this study is to focus on a simple and low-cost method to transform waste cigarette filters into cellulose diacetate (CDA) films, which can be used in packaging films. Furthermore, waste must be recycled in order to be reused. In this paper, cellulose diacetate films derived waste cigarette filters with different volume ratios of glycerol, (0.25, 0.50, 0.75, and 1.00 mL) glycerol as the plasticizer (CDAG) have been successfully prepared by the solvent evaporating method of the CDA and CDAG films were determined. The physical parameters, the mechanical properties, the degree of swelling and water uptake. The prepared CDA films were characterized using XRD, SEM, FT IR and TG DTA analysis. From the FT IR analysis, the characteristic absorption peaks of CDA and CDAG films clearly showed that the two polymers were well mixed. According to TG-DTA analysis, the thermal stability of the CDA blended film was found to be slightly higher. The antimicrobial activity of CDA and CDAG films was investigated by agar-disc diffusion method. Subsequently, the biodegradable nature of the prepared CDA and CDAG films was studied through the soil burial test. Finally, the prepared CDA and CDAG films can be used as packaging materials.

Keywords: Cigarette waste cellulose diacetate, glycerol, antimicrobial activity, biodegradable nature

Introduction

Cigarette waste has polluted the environment due to the non-biodegradability and toxic substances found in cigarette filters. The reuse of cigarette waste is a hot topic in today's society. Many countries and regions have proposed relevant policies and methods for trying to collect waste cigarettes, but reusing waste cigarettes remains a challenge (Zhang *et al.*, 2020). Cellulose is a linear carbohydrate polymer with long chains of β -D glucopyranose units linked by β -1,4-glycosidic bonds. It is considered to be one of the most abundant molecules in the biosphere. As one of the most commercially important cellulose derivatives, cellulose acetate (CA) is widely used in the manufacture of plastics, textiles, filter tows, films, or membranes (Arroyo *et al.*, 2020). Cellulose acetate, an organic ester, is a bio-based polymer with excellent mechanical properties. Its general properties can be adjusted by adding small-molecule plasticizers that are also needed for treatment. Over the last few decades, various types of plasticizers based on glycols, phthalates, acetates, and citrates have been incorporated into CA (Erdmann *et al.*, 2021). Cellulose and its derivatives have been used in a wide range of applications due to their abundant sources, excellent biodegradability, and effective renewability. Cellulose acetate is one of the most important cellulose esters and is widely used in the manufacturing industry owing to its excellent all-around properties (Boulven *et al.* 2019).

CA is mainly synthesized via acetylation and hydrolysis reactions, and it can result in a desirable degree of substitution (DS). Based on its DS value, CA is typically classified as cellulose diacetate (CDA, DS =2.2–2.7) or cellulose triacetate (CTA, DS=3) (Wang *et al.*, 2017). Traditional plasticization of the CDA has been performed using traditional plasticizers such as phthalates, glycerol derivatives, and phosphates. This plasticization often leads to problems caused by the bleeding of plasticizers with harmful properties and decomposition products. In this regard,

¹ Department of Chemistry, University of Yangon, Myanmar

² Department of Chemistry, University of Yangon, Myanmar

there have been several attempts to use aliphatic polyesters as a plasticizer for cellulose acetate (CA). With this situation in mind, we recently sought to find new plasticizers and plasticization processes that could provide biodegradable thermoplastic polymers from CA (Lee and Shiraishi, 2001). Plasticizers can lower the glass transition temperature of CA and reduce the intramolecular force between polymer chains, resulting in a softer and more flexible polymer matrix (Cindradewi *et al.*, 2021). To improve the processing of CA, some studies have explored several eco-friendly plasticizers such as Triacetin (TA), Triethyl citrate (TC), glycerol, and polyethylene glycol (PEG) (Teixeira *et al.*, 2021). These plasticizers are biodegradable, non-toxic, and have been approved as plasticizers for many polymers. TA and TC are two of the most common eco-friendly plasticizers that have been used for CA. TA and CA share the same side functional groups: acetyl groups. It has been demonstrated that TC can improve the stiffness and brittleness of CA films (Lee and Shiraishi, 2001). The addition of plasticizers to the CA matrix reduces tensile strength (Phuong *et al.*, 2014). Therefore, it could impede the function of CA bio-plastics in specific industries.

Materials and Methods

Waste cigarettes were collected from domestic waste. Glycerol and glacial acetic acid were purchased from the British Drug House (BDH) Chemical Ltd., England. All of the chemicals used in this study were of analytical grade. In all investigations, the recommended standard methods and techniques involving both conventional and modern methods were used.

Preparation of Cellulose Diacetate (CDA) Film

The CDA films were prepared via the solution casting method. Firstly, collected waste cigarette filters were washed with ethanol and hot water several times and then dried at 60 °C. Secondly, the above waste cigarette filters were dissolved in glacial acetic acid at a ratio of 1:15 (w/w) and then treated using an overhead stirrer for 4 h to form a homogeneous emulsion. Subsequently, the different volumes of 0.25, 0.50, 0.75, and 1.00 mL glycerol were added to above emulsion. In addition, the sample without glycerol was used as a comparison. Finally, the obtained solution was poured onto a melamine plate and dried at room temperature to form CDA films. In this work, as-prepared samples were denoted as CDA, CDAG-0.25, CDAG-0.50, CDA-0.75, and CDAG-1.00 according to the volume of glycerol, respectively.

Physical Parameter Measurement of CDA and CDAG Solutions

Determination of pH

Each sample solution was placed into separate beakers. The pH of the solution was measured by using a pH meter at room temperature (Htwe *et al.*, 2021).

Determination of specific gravity

A SG density bottle (50 cm³) was washed and cleaned with distilled water, thoroughly dried and subsequently weighed. Then the SG bottle was filled with distilled water at room temperature. The stopper was firmly inserted in the bottle, and excess distilled water exiting from the capillary of the stopper was wiped carefully with a piece of tissue paper. Then the bottle containing water was weighed. In order to determine the specific gravity of the sample, the bottle was thoroughly dried and filled with the different CDA solutions at room temperature. The excess solution from the capillary was wiped with the piece of tissue paper and weighed. The specific gravity of different samples was calculated using the following Equation (1) (Htwe *et al.*, 2021).

$$\text{Specific gravity (SG)} = \frac{W_3 - W_1}{W_2 - W_1} \times \text{density of liquid} \quad (1)$$

where, W_1 is the weight of the density bottle in grams, W_2 is the total weight of the density bottle with distilled water in grams and W_3 is the total weight of the density bottle with sample solution in grams.

Determination of viscosity

About 50 cm³ of sample solution was placed into the viscometer cup. The solution was kept in a constant temperature bath at 30 °C and was measured the rotational viscosity (cPs) with VISCO viscometer (Htwe *et al.*, 2021). A VISCO 6800-E07 viscometer, ATAGO, Japan was used for determining the viscosity.

Determination of transparency

The transparency of edible film was measured using a UV spectrophotometer at a wavelength of 550 nm. Film transparency is measured using the method of Bao *et al.* (2009) and the transparency of CDA and CDAG films was calculated using the formula (2):

$$T = A_{550}/x \quad (2)$$

where, T is transparency, A_{550} is absorbance at a wavelength of 550 nm, and x is film thickness (mm).

Determination of Physicomechanical Properties

The tensile strength, elongation at break and tear strength of the samples were measured on the Tensile testing machine (Hours Field 5000E), Cutter (Wallace) at room temperature with the rate of moveable jaw 100 mm/min according to JIS K 7127 (1987). Three samples were measured and average values were reported (Htwe *et al.*, 2013).

Determination of Water Uptake (%)

The films to be tested were cut into 1" × 1" size. The cut films were immersed in distilled water at room temperature for the specified period of time. The films were removed from distilled water in a beaker, blotted gently with tissue paper, weighed, and then put back into beaker for the next measurement. The water uptake of different samples was calculated using the Equation (3) (Htwe *et al.*, 2021).

$$\text{Water uptake (\%)} = \frac{W_2 - W_1}{W_1} \times 100 \% \quad (3)$$

where, W_1 is the weight of completely dried sample and W_2 is the weight of a swelled sample in distilled water at room temperature for 1 hour.

Determination of Degree of Swelling

The films to be tested were cut into 1" × 1" size. The films were immersed in distilled water at room temperature for the specified period of time. The films were removed from distilled water in a beaker, blotted gently with tissue paper, weighed, and then put back into the beaker for the next measurement. The procedure was continued until no more water was absorbed. Based on these values, swelling (%) was determined. Each experiment was replicated three times. The degree of swelling was determined according to Equation (4).

$$\text{Degree of swelling (\%)} = \frac{W_s - W_d}{W_s} \times 100 \% \quad (4)$$

where, W_s and W_d represent the weight of the films after and prior to immersion. All the experiments were carried at room temperature.

Characterization

The surface morphology of CDA materials was studied using SEM (JOE-JSM-5610 LV model, Japan). SEM images of samples were collected under an accelerating voltage of 5 kV. A Fourier transform infrared spectrophotometer (Shimadzu, Japan) was used. The resolution was 4 cm^{-1} with 64- time scanning, and the scanning was performed in the range of $4000\text{--}400 \text{ cm}^{-1}$. The X-ray diffraction (XRD) measurements of the different CDA films were recorded using a Shimadzu 8000 X-ray diffractometer (Shimadzu, Japan) with a detector operating under a voltage of 40.0 kV and a current of 30.0 mA using Cu $K\alpha$ radiation ($\lambda = 0.15418 \text{ nm}$). The recorded range of 2θ was $5\text{--}40^\circ$, and the scanning speed was $6^\circ/\text{min}$. The thermal properties of CDA films were characterized by thermogravimetric analysis (TGA) on a thermogravimetric analyzer (Rigaku Thermoplus TG 8120) in the range of $30\text{--}600^\circ\text{C}$ at a heating rate of $10^\circ\text{C min}^{-1}$ under N_2 flow.

Antimicrobial activity of CDA Films

The antimicrobial activity of CDA film was carried out by agar disc diffusion method at Patheingyi University, Myanmar. Eight microorganisms, namely *Escherichia coli*, *Candida albicans*, *Bacillus subtilis*, *Staphylococcus aureus*, *Pseudomonas fluorescens*, *Agrobacterium tumefaciens*, *Bacillus pumilus*, and *Micrococcus luteus* were used for this test.

Biodegradable Nature of CDA Films

Biodegradation of prepared CDA film was determined by soil burial test, and weight loss and morphology were examined. The films were cut into $1'' \times 1''$ dimensions. The films were then accurately weighed and buried in soil at a depth of 5 cm. They were taken out from the soil at an interval of 2 weeks.

Results and Discussion

Physical Parameters of CDA and CDAG Solutions

Figure 1 shows the physical parameters (pH, specific gravity, and refractive index) of different CDA solutions. From the value of pH, it can be observed that different CDA solutions are slightly acidic solutions in the range of 3.13 to 3.50. The specific gravity of different CDA solutions is in the range of 1.12 to 1.14. It can be seen that there are no significant changes in specific gravity. The refractive indices of different CDA solutions are around 1.38. The viscosity of CDA solution is 980.4 cPs for CDA, 915.2 cPs for CDAG-0.25, 912.8 cPs for CDAG-0.50, 912.8 cPs for CDAG-0.75, and 1020.1 cPs for CDAG-1.00 at 25°C . Thus, all physical parameters of CDAG solutions showed slightly different values.

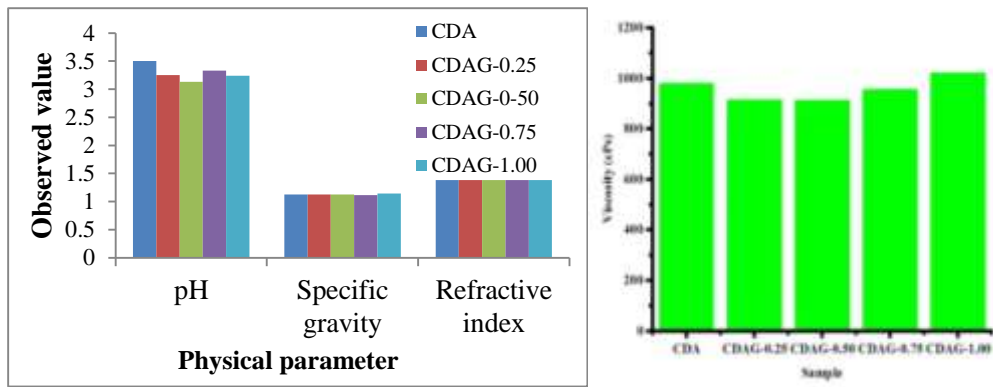


Figure 1. Physicochemical properties of CDA and CDAG solutions

Transparency of CDA and CDAG Films

Transparency is an aesthetic for marketing edible films. Transparency values represent the level of clarity of the films produced (Mustapa *et al.*, 2017). The results of the analysis presented in Figure 2 show that glycerol concentration had a significant effect on the transparency of edible films. The average transparency of CDA film in each treatment is CDAG0 (11.1 %), CDAG0.25 (11.6 %), CDAG0.5 (10.9 %), CDAG0.75 (10.3 %), and CDAG1 (9.8 %).

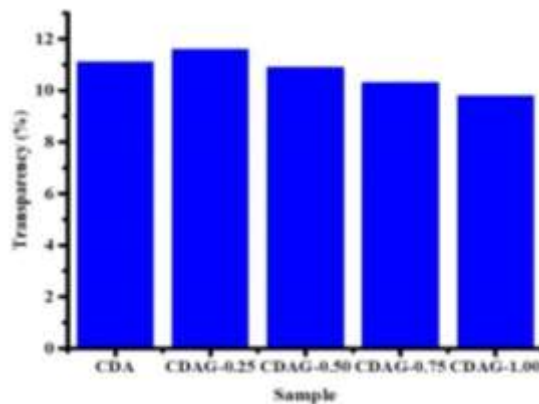


Figure 2. The transparency percentage of CDA and CDAG films

Physicomechanical Properties of CDA and CDAG Films

The physicomechanical properties in terms of tensile strength, elongation at break (%), and tear strength are important parameters which reveal the nature of films. The physicomechanical properties of different CDA films are presented in Figure 3. The thickness of CDA films is in the range of 0.01 mm to 0.05 mm. Tensile strength increased from 8.3 MPa to 52.5 MPa. As shown in figure 3(a), the tensile strengths of the CDA, CDAG-0.25, CDAG-0.50, CDAG-0.75, and CDAG-1.0 films were 8.3, 15, 28, 39.2, and 52.5 MPa, with elongation at break values of 3, 4.2, 8, 5.2, and 6 %, respectively. It can be seen that the tensile strength of all CDAG-0.25, CDAG-0.5, CDAG-0.75, and CDAG-1.0 films was much higher than that of CDA film, and the elongation at break of the former was longer. The sample of CDAG-1.0 with an elongation at break of 6 % had a maximum tensile strength of 52.5 MPa. Interestingly, the tensile strength declined sharply, although the elongation at break continued to increase when the content of glycerol was increased. These results demonstrate that the flexibility of as-prepared films can be improved with an increase in glycerol content. The tear strength is another mechanical property of the nature of films. Figure 3(b) shows the profile of tear strength versus glycerol content. It was found that the tear strength of CDAG film increased significantly and progressively from 0 to 0.75 % v/v glycerol content.

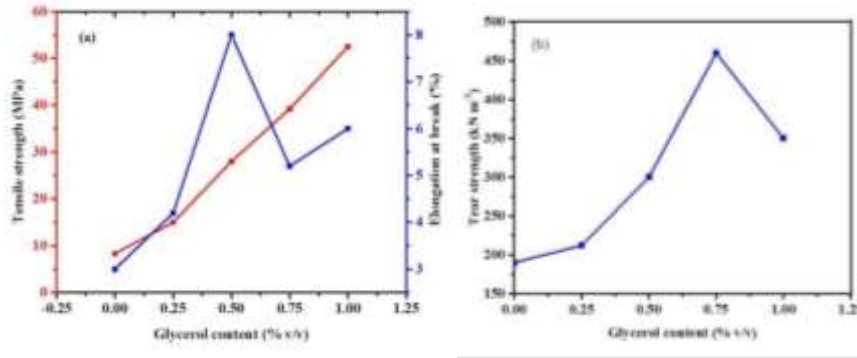


Figure 3. (a) Tensile strength and elongation at break and (b) tear strength of CDA and CDAG films as a function of glycerol concentration

Water Uptake (%)

The degree of water uptake was investigated with increasing immersion time. It was found that the water uptake of all samples was increased by increasing the glycerol content at 50 min. When a film was used as a biodegradable material, one of the most important parameters was water uptake. The water uptake was the amount of water entrapped in the matrix, including bound water (Htwe *et al.*, 2013). Figure 4 shows the water uptake percent for CDAG films. The water uptake of different CDAG films was significantly different according to the various ratios of glycerol compared to those of CDA films. CDAG 0.75 had the highest degree of water uptake content (85.71%) at 50 minutes. The water uptake degree of every CDAG film increased with increasing time. The water uptake may impart stickiness and durability.

Aspect of Degree of Swelling (%)

The degree of swelling of CDAG films is shown in Figure 5 as a function of immersion time in distilled water at room temperature. For a given blended film composition, the degree of swelling mostly increased with increasing immersion time. It can also be observed that the degree of swelling increased with increasing glycerol content in the blended film. The maximum value for the degree of swelling of the CDAG 0.75 film was 45 % at 50 minutes.

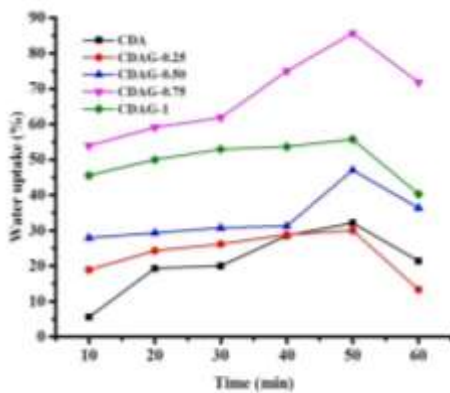


Figure 4. Degree of water uptake percent of CDA and CDAG as a function of contact time

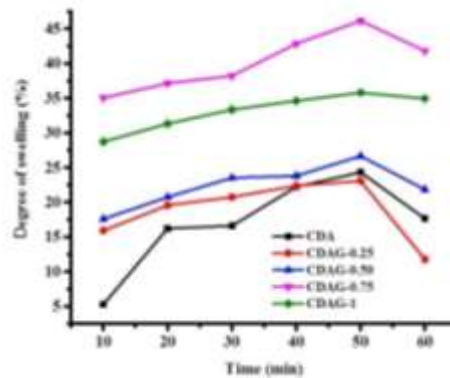


Figure 5. Degree of swelling percent of CDA and CDAG as a function of contact time

Characterization

In this study, CDA films with different ratios of glycerol were chosen and characterized by FT IR and TG-DTA analysis. After that, antimicrobial properties and biodegradable nature of the chosen blend films were determined by the agar disc diffusion method and the soil burial method.

FT IR spectroscopy

Figure 6 depicts the FTIR spectra of CDA, CDAG-0.25, CDAG-0.50, CDAG-0.75, and CDAG-1.00. The CDA film had several distinguishing bands at approximately 1735 cm⁻¹, 1367 cm⁻¹, 1231 cm⁻¹, and 1023 cm⁻¹ (Wang *et al.*, 2017). These bands correspond to the stretching vibration of C=O in acetyl groups, the symmetric bending vibration of C-H in methyl groups, the asymmetric stretching vibration of C-O-C in ester groups, and the stretching vibration of C-O-C in the pyranose ring (Rambaldi *et al.*, 2014; Vallejos *et al.*, 2012). Because glycerol is an alcohol with a chemical structure that contains CH and OH groups, its incorporation into cellulose acetate may have increased the interactions between the two compounds in the bands that represent these attributes. Because the plasticizer's OH group is available for possible interactions, hydrogen bonds between the OH groups of CA and glycerol may form. In contrast, glycerol has two more OH groups that will not be available for interactions. As a result, the prominent OH band could be related to the increased amount of OH in the film as a result of the glycerol addition (Goncalves *et al.*, 2019). It was found that adding glycerol increased the intensity of the band at 3319 cm⁻¹, corresponding to the stretching vibration of O-H groups. Because glycerol contains O-H groups, hydrogen bonds may form between glycerol and the CDA film. Furthermore, O-H groups that are not involved in glycerol interactions result in a higher content of O-H groups in the CDA film (David and Gong, 2018).

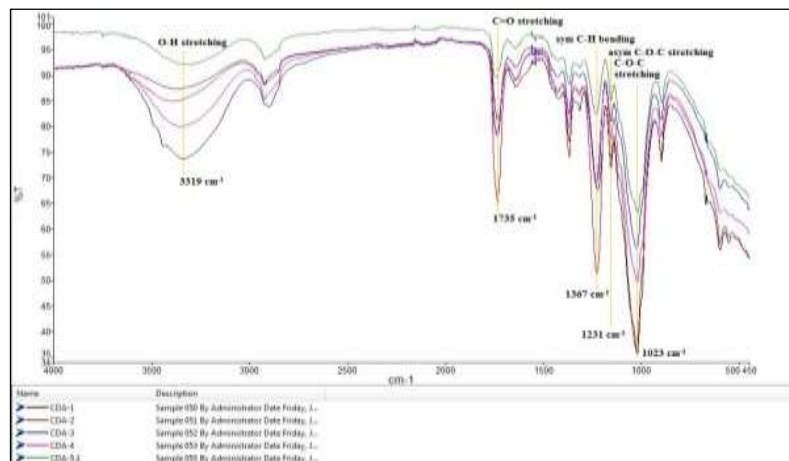


Figure 6. FT IR spectra of CDA and CDAG films

Table 1. The Wavenumber Assignment of CDA and CDAG Films

Samples	C-C & C-H bend	C-O-C stretch	Asym C-O-C stretch	Symmetric C-H bend	C=O stretch	CH stretch	OH stretch
CDA	902.24	1023.80	1227.60	1370.60	1731.60	2904.30	3333.30
CDAG0.25	898.67	1023.80	1224.00	1370.60	1735.20	2922.10	3383.30
CDAG0.50	898.67	1023.80	1227.60	1367.00	1735.20	2925.70	3354.70
CDAG0.75	898.67	1020.20	1234.70	1370.60	1738.80	2918.60	3347.60
CDAG1.0	895.10	1023.80	1231.10	1367.00	1735.20	2922.10	3319.00

* Wang *et al.* 2017 ; Rambaldi *et al.* 2014 ; Goncalves *et al.*, 2019

X-ray diffraction analysis

The XRD patterns of CDA, CDAG-0.25, CDAG-0.5, CDAG-0.75, and CDAG-1.0 are shown in Figure 7. There was an obvious peak at 21.9 for CDA/glycerol films, and the CDA peak at 21.9 was much weaker. This research shows that a single CDA film has low crystallinity and that glycerol can improve the crystallinity of composite films. Glycerol can disrupt the CDA chain arrangement and form hydrogen bonds between them. Figure 8 depicts an illustration of the glycerol-CDA reaction process. Glycerol disrupts CDA chain arrangement, and then-OH groups in glycerol combine with oxygen-containing groups in CDA chains to form hydrogen bonds (Zhang *et al.*, 2020).

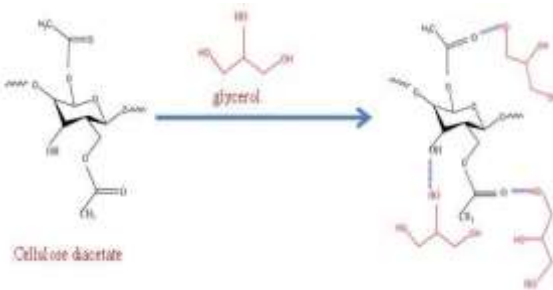
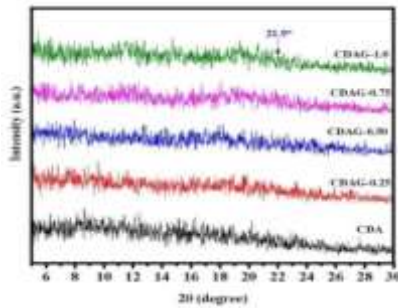


Figure 7. XRD patterns of different CDAG films

Figure 8. The illustration for the reaction of glycerol and CDA chains (Zhang *et al.*, 2020)

SEM Analysis

The morphology of the prepared CDA, CDAG-0.25, CDAG-0.50, CDAG-0.75 and CDAG-1.0 was examined using scanning electron micrographs (SEM). The surfaces of CDA, CDAG-0.25, CDAG-0.50, CDAG-0.75, and CDAG-1.0 have a generally smooth morphology, as shown in Figures 9a-e. It was found that CDA film had a smoother surface than other films (Figure. 9a). However, some small pores and depressions were found on the surface of CDA/glycerol films (in Figure. 9b-e). Furthermore, as the glycerol content increased from 0.25 % to 1.0 %, the number of pores also increased. The surface morphologies of the films changed slightly when the glycerol content exceeded 1.0%. This is because glycerol-adsorbed water evaporates during the drying process of CDA films (Zhang *et al.*, 2020).

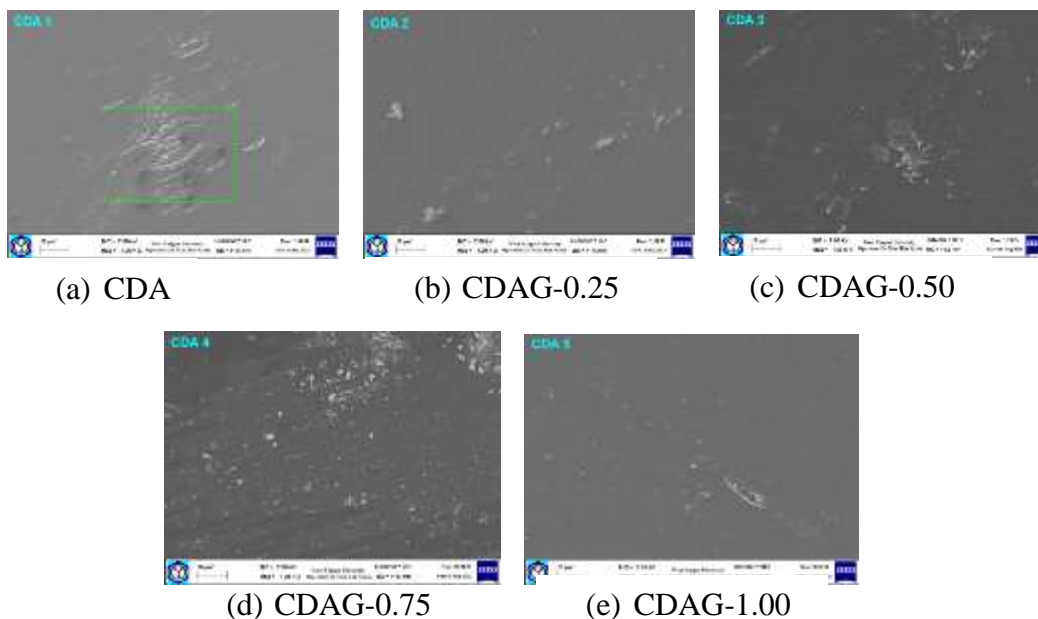


Figure 9. SEM images of CDA and different CDAG films

TG-DTA analysis

The thermal stability of CDA films with varying glycerol ratios (CDAG-0.25, CDAG-0.50, CDAG-0.75, and CDAG-1.00) was investigated using thermogravimetric analysis, as shown in Figures 10(a) and (b). As seen in Figures 10(a) and (b), the thermal stability of as-prepared CDAG films was assessed by TGA and DTG. As shown in Figure. 10(a), the thermal decomposition of CDA film includes two main stages. Firstly, CDA film has a total weight loss of 2.61 % in the range of 39 °C to 150 °C. This is due to evaporation of water. When the temperature exceeded 280 °C, the polymer chains for the CDA began to decompose, losing 83.88% of their weight, resulting in exothermic peaks in Figure 9(b) at 347 °C and 503 °C. Figure 10(a) shows the thermal degradation of CDAG films, which behave similarly to CDA films, in three stages: the first stage shows a total weight loss of 5.85% for CDAG-0.25, 4.26% for CDAG-0.50, 5.80% for CDAG-0.75, and 4.69% for CDAG-1.00 in the range of 39 °C to 150 °C. This is due to the evaporation of water on the film and moisture in glycerol. In the second stage, the loss in weight of 82.42 % for CDAG-0.25, 80.35 % for CDAG-0.50, 73.71 % for CDAG-0.75 and 79.60 % for CDAG-1.00 were observed to take place within the temperature range of 288 °C to 380 °C. Sharp exothermic peaks are shown in Figure 9(b) at 363 °C (CDAG-0.25), 347 °C (CDAG-0.50), 336 °C (CDAG-0.75), and 353 °C (CDAG-1.00). This is due to the thermal degradation of glycerol molecules. According to the CDAG curves in Figure 10(a), the third stage temperature range between 380 °C and 600 °C lost 4.76% for CDAG-0.25, 12.75% for CDAG-0.50, 12.43% for CDAG-0.75, and 9.52% for CDAG-1.00, corresponding to exothermic peaks at 456 °C (CDAG-0.25 in Figure 10(b)) and 486 °C (CDAG-0.50 in Figure 9(b)), 446 °C (CDAG-0.75 in Figure 10(b)) and 486 °C (CDAG-1.00 in Figure 10(b)). This is due to the thermal degradation of CDA chains. Interestingly, it was found that the residual weight of CDA films after adding glycerol increased. However, the weight loss of CDAG films was greater than that of CDA film before 300 °C, which was attributed to the evaporation of water in glycerol. The added plasticizer reduces the intermolecular forces between CDA chains (Zhang *et al.*, 2020).

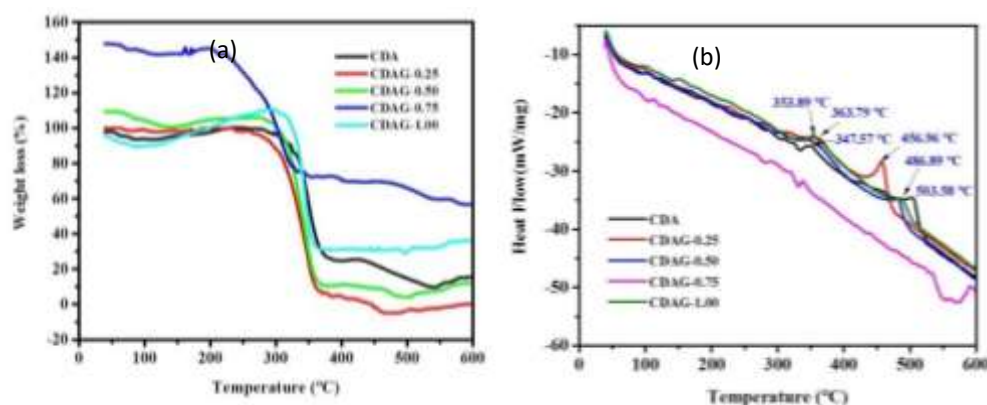


Figure 10. (a)TG curves (b) DTA curves for CDA and CDAG films

Antimicrobial Activity of CDA and CDAG Film

Pure CDA and CDAG films were screened for antimicrobial activity against eight different pathogenic microbes (Figure 11). It was observed that all of the films did not show any antimicrobial activity except *Bacillus subtilis* and *Escherichia coli* for CDA film and *Escherichia coli* for CDAG-0.25 film against all of the microorganisms tested. Eight microorganisms with the

inhibition zone diameter ranging below 10 mm for all of the films. According to results, CDA and CDAG-0.25 films possessed pronounced activity against *Bacillus subtilis*, and *Escherichia coli*.

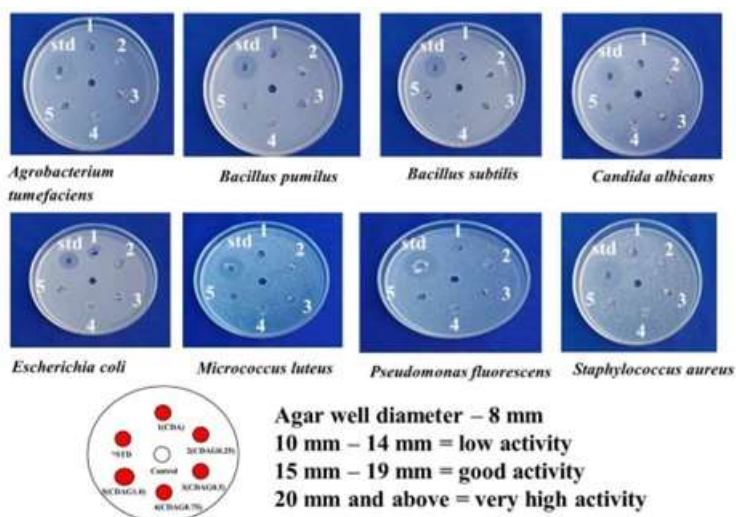


Figure 11. Photo records showing inhibition zone due to the effect of CDA and CDAG films

Biodegradation test by soil burial

The biodegradability of CDA and CDAG films was tested by the soil burial method under natural soil condition (pH = 6.95). As described above, environmental effects mentioned in this work are moisture and soil which may be favorable conditions for the microbial growth (Gu *et al.*, 2000). Soil burial is a traditional method to test samples for degradation because of its similarity to actual condition of waste disposal. Uniformly sized samples were buried in the soil from waste disposal. The physical appearances of blended films after buried in the soil are shown in Figure 12.

Figure 12 shows biodegradation nature of different CDAG films within one month interval. There, the weight loss was about 10.3%, 14.1 %, 10.2%, 15.2 % and 14.4 % of CDA, CDAG-0.25, CDAG-0.50, CDAG-0.75, and CDAG-1.00 after 2nd week. After 4 weeks, it was found that the weight loss was about 84.2 %, 89.6 %, 90.2 %, 91.0 % and 90.6 % of CDA, CDAG-0.25, CDAG-0.50, CDAG-0.75, and CDAG-1.00. It can be seen with slight degradation, before 2 weeks. However, quite deformation of CDA film appeared after 2 weeks. From this investigation, it was expected that these films would be degradable in soil in more than one month. One of the objectives of the development of CDA is to remove easy-to-throwaway materials from degradable plastic to alleviate the waste disposal problem through environmental degradation.

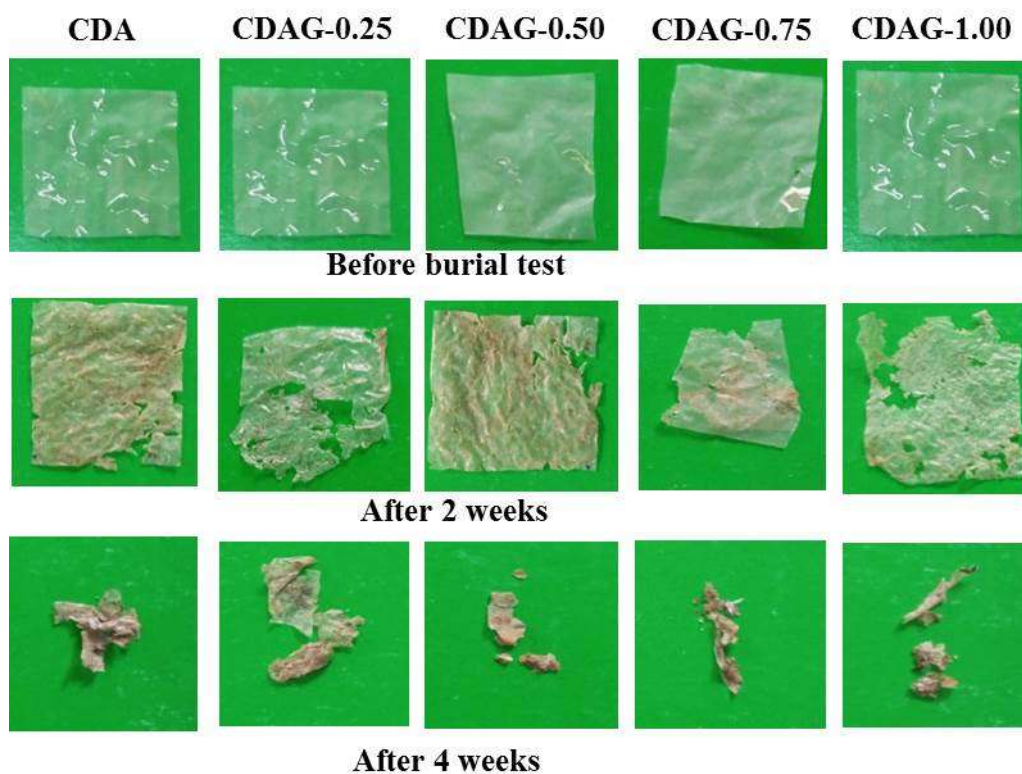


Figure 12. The physical appearances of CDA and CDAG films

Conclusion

Waste cigarette filters were recycled to prepare an excellent cellulose diacetate film. Glycerol significantly improved the mechanical properties of CDA films. When the glycerol volume content was 1 mL, the as-prepared film with a 6% elongation at break had the highest tensile strength of 52.5 MPa. Furthermore, the swelling and water uptake of the film demonstrated a higher degree of hydration, as measured by swelling and water uptake, which can be varied by varying the volume percentage of glycerol in the film matrix. FT IR and XRD analysis indicated that hydrogen bonds were formed between CDA chains and glycerol. From TG-DTA analysis, CDAG films exhibited better thermal stability. SEM images revealed that glycerol caused the formation of small pores in films, and the number of pores increased as the glycerol content increased. The CDA and CDAG films were tested for their antimicrobial activities by using the agar disc diffusion method. It can be noted that all of the microbial agents that came into contact with films did not possess pronounced activity. By using the soil burial techniques, it was found that a significant deformation of CDA and CDAG films had occurred at 4 weeks. According to these results, CDA and CDAG films can be made from used cigarette filters and are a good replacement for packaging film.

Acknowledgements

The authors owe their gratitude to Professor Dr Ni Ni Than, Head of Department, Department of Chemistry, University of Yangon, Yangon, Myanmar, for her stimulating suggestions.

References

- Arroyo, F. D., C. F. Guerrero, and U. L. Silva. (2020). "Thin Films of Cellulose Acetate Nanofibers from Cigarette Butt Waste". *Progress in Rubber Plastics and Recycling Technology*, vol. 36(1), pp. 3-17
- Bao, S., S. Xu, and Z. Wang. (2009). "Antioxidant Activity and Properties of Gelatin Films Incorporated with Tea Polyphenol-Loaded Chitosan Nanoparticles". *Journal of the Science of Food and Agriculture*, vol. 89, pp. 2692-2700
- Boulven, M., G. Quintard, A. Cottaz, C. Joly, A. Charlot, and E. Fleury. (2019). "Homogeneous Acylation of Cellulose Diacetate: Towards Bioplastics with Tuneable Thermal and Water Transport Properties". *Carbohydrate Polymers*, vol. 206, pp. 674-684
- Cindradewi, A. W., R. Bandi, C. W. Park, J. S. Park, E. A. Lee, J. K. Kim, G. J. Kwon, S. Y. Han, and S. H. Lee. (2021). "Preparation and Characterization of Cellulose Acetate Film Reinforced with Cellulose Nanofibril". *Polymers*, vol. 13(2990), pp. 1-14
- David, B.K.L., and H. Gong. (2018). "Highly Stretchable and Transparent Films Based on Cellulose". *Carbohydr. Polym.*, vol. 201, pp. 446-453
- Erdmann, R., S. Kabasci, and H. P. Heim. (2021). "Thermal Properties of Pasticized Cellulose Acetate and Its Relaxation Phenomenon". *Polymers*, vol. 13(1356), pp. 1 – 14
- Goncalves, S. M., D. C. dos Santos, J. F. G. Motta, R. R. dos Santos, D. W. H. Chavez, and N. R. de Melo. (2019). "Structure and Functional Properties of Cellulose Acetate Films Incorporated with Glycerol". *Carbohydrate Polymers*, vol. 209, pp. 190-197
- Htwe, A. T., M. Htwe, S. Maung, and M. N. Tun. (2021). "Study on Biodegradable and Antimicrobial Properties of Biowaste Chitin-Polyvinyl Alcohol Blended Film". *ASEAN Engineering Journal*, vol. 11(3), pp. 127-139
- Htwe, A. T., S. Tun, K. A. May, and K. M. Naing. (2013). "Studies on preparation, characterization and application of pH-sensitive biodegradable chitosan-polyvinyl alcohol hydrogel". *Jour. Myan. Acad. Arts & Sc*, vol. XI(1), pp. 127-140
- Lee, S. H., and N. Shiraishi. (2001). "Plasticization of Cellulose Diacetate by Reaction with Maleic Anhydride, Glycerol, and Citrate Esters during Melt Processing". *Journal of Applied Polymer Science*, vol. 81, pp. 243-250
- Phuong, V. T., S. Verstichel, P. Cinelli, I. Anguillesi, M. B. Coltelli, and A. Lazzeri. (2014). "Cellulose Acetate Blends- Effect of Plasticizers on Properties and Biodegradability". *J. Renew. Mater.*, vol. 2, pp. 35-41
- Rambaldi, D.C., C. Suryawanshi, C. Eng, and F.D. Preusser. (2014). "Effect of Thermal and Photochemical Degradation Strategies on the Deterioration of Cellulose Diacetate". *Polym.Degrad. Stab.*, vol. 107, pp. 237-245
- Teixeira, S. C., R. R. A. Silva, T. V. Oliveira, P. C. Stringheta, M. R. M. R. Pinto, and N. D. F. F. Soares. (2021). "Glycerol and Triethyl Citrate Plasticizer Effects on Molecular, Thermal, Mechanical, and Barrier Properties of Cellulose Acetate Films". *Food Bioscience*, vol. 42(101202), pp. 1-10
- Vallejos, M.E., M.S. Peresin, and O.J. Rojas. (2012). "All Cellulose Composite Fibers Obtained by Electrospinning Dispersions of Cellulose Acetate and Cellulose Nanocrystals". *J. Polym. Environ.*, vol. 20, pp. 1075-1083
- Wang, W., T. Liang, H. Bai, W. Dong, and X. Liu. (2017). "All Cellulose Composites Based on Cellulose Diacetate and Nanofibrillated Cellulose Prepared by Alkali Treatment". *Carbohydrate Polymers*, vol. 179, pp. 297-304
- Zhang, Q., C. Fang, Y. Cheng, J. Chen, Z. Huang, and H. Han. (2020). "Construction and Properties of Cellulose Diacetate Film". *Cellulose*, vol. 27, pp. 8899-8907